Bulletin of the Geological Society of Finland, Vol. 87, 2015, pp 25–45, http://dx.doi.org/10.17741/bgsf/87.1.002

Geochronology of the Suomenniemi rapakivi granite complex revisited: Implications of point-specific errors on zircon U-Pb and refined λ_{87} on whole-rock Rb-Sr

O.T. Rämö[1)*] and I. Mänttäri[2)]

[1)] *Department of Geosciences and Geography, Division of Geology and Geochemistry (DiGG), P.O. Box 64, FI-00014 University of Helsinki, Finland*

[2)] *Geological Survey of Finland, P.O. Box 96, FI-02151 Espoo, Finland*

Abstract

Multi-grain isotope dilution and secondary ion microprobe zircon U-Pb as well as whole-rock Rb-Sr isotope dilution data on the late Paleoproterozoic Suomenniemi rapakivi granite complex (exposed on the northern flank of the Wiborg batholith in southeastern Finland) are discussed in the light of point-specific errors on Pb/U and proposed new values of the decay constant of ^{87}Rb, λ_{87}. U-Pb zircon data on hornblende granite and biotite granite of the main metaluminous-marginally peraluminous granite fractionation series of the Suomenniemi batholith indicate crystallization in the 1644-1640 Ma range, with a preferred age at 1644±4 Ma. A cross-cutting hornblende-clinopyroxene-fayalite granite is probably slightly younger, as are quartz-feldspar porphyry dikes (1634±4 Ma) that cut both the main granite series and the metamorphic Svecofennian country rocks of the Suomenniemi batholith. Recalculation of whole-rock Rb-Sr data published on the main granite series of the batholith by Rämö (1999) implies errorchron ages of 1635±10 Ma and 1630±10 Ma and a magmatic ^{87}Sr/^{86}Sr$_i$ of 0.7062±0.0024. This relatively high initial ratio is indicative of a major Proterozoic crustal source component in the granites of the batholith. The main granite series of the batholith probably cooled relatively rapidly to and below the closure temperature of the Rb-Sr isotope system, with little subsequent subsolidus adjustment. The three discrete silicic magmatic phases of the batholith (the main granite series, the hornblende-clinopyroxene-fayalite granite, and the quartz-feldspar porphyry dikes) were all probably emplaced before the main volume of rapakivi granite (the Wiborg batholith proper) in southeastern Finland. The Suomenniemi batholith thus represents an early magmatic precursor to the classic Wiborg batholith and was emplaced clearly before the massive rise of isotherms associated with the ascent and crystallization of the magmas that formed the bulk of the Wiborg batholith system.

Keywords (GeoRef Thesaurus, AGI): granites, rapakivi, batholiths, absolute age, U/Pb, zircon, geochemistry, isotopes, Rb/Sr, thermal ionization mass spectroscopy, secondary ion mass spectroscopy, Proterozoic, Suomenniemi, Finland

*Corresponding author e-mail: tapani.ramo@helsinki.fi

Editorial handling: Jussi S. Heinonen (jussi.s.heinonen@helsinki.fi)

1. Introduction

The classic Wiborg rapakivi granite batholith of southeastern Finland and its satellite intrusions were emplaced into the Paleoproterozoic Svecofennian metamorphic crust as a sequence of discordant, epizonal complexes that are overwhelmingly silicic but also include members of basic and rare intermediate rocks (Haapala & Rämö, 1990; Rämö & Haapala, 2005). The main igneous body – the Wiborg batholith proper – is ~ 150 km in its current exposed diameter, with one-third concealed under the Gulf of Finland and underneath Neoproterozoic-Paleozoic sedimentary rocks in the south. The Wiborg batholith probably constitutes a relatively thin (~ 10-15 km) intrusion (as compared to its diameter), exposed and beheaded by extensional tectonics well before the Phanerozoic Eon (Korja & Elo, 1990; Kohonen & Rämö, 2005; see also Kohonen, 2015). On the northern flank of the batholith, two prominent satellite igneous bodies are found (Fig. 1): the Suomenniemi complex, which is composed of an extensive granite fractionation series, associated silicic and basic dike rocks, and minor anorthosite and peralkaline alkali-feldspar syenites (Pipping, 1956; Simonen & Tyrväinen, 1981; Sundsten, 1985; Rämö, 1991), and the Ahvenisto complex, which comprises, besides granites, a major body of massif-type anorthosite and associated mafic intermediate (monzodioritic) rocks as well as silicic and basic dikes (Savolahti, 1956; Johanson, 1984; Alviola et al., 1999; Heinonen et al., 2010a). U-Pb mineral geochronological work performed on the rapakivi granites of southeastern Finland shows that the Wiborg batholith and its satellite bodies were emplaced at the end of the Paleoproterozoic, mainly between 1650 Ma and 1625 Ma (Vaasjoki et al., 1991). Taking into account of the external analytical errors of better than 0.25 %, U-Pb zircon ages of various plutonic and hypabyssal rocks of the Wiborg batholith imply a minimum duration of the magmatism of 20 m.y. (from 1642 Ma to 1622 Ma) (Rämö et al., 2014). Geochronological data also suggest that the granite bodies on the northern flank of the Wiborg batholith are older than the main batholith (Vaasjoki et al., 1991; Rämö et al., 2014).

The Suomenniemi complex due north of the main Wiborg batholith (Fig. 1) has been the subject of extensive geochronological and other isotope geochemical work. Granites, a minor massif-type anorthosite occurrence, sodic peralkaline syenites, and silicic and basic dikes have been analyzed using various isotopic methods, with U-Pb mineral data being available for 11 samples (Siivola, 1987; Vaasjoki et al., 1991), Sm-Nd whole-rock and Pb-Pb whole-rock and alkali feldspar data for, in total, 29 samples (Rämö, 1991), Rb-Sr whole-rock data for ten samples (Rämö, 1999), oxygen-in-zircon (laser-fluorination) data for two samples (Elliott et al., 2005), and Lu-Hf-in-zircon data for two samples (Heinonen et al., 2010b). These results imply an overall emplacement of the granites of the batholith at ~ 1640 Ma and a major Paleoproterozoic crustal component in them (ε_{Ndi} of -3 to -1; neodymium T_{DM} model ages of ~ 2.1 Ga; Stacey & Kramers, 1975, second-stage $^{238}U/^{204}Pb$ of 8.73 to 8.75; $^{87}Sr/^{86}Sr_i$ of ~ 0.7066; $\delta^{18}O$-in-zircon of 8.1‰; ε_{Hfi} of ~ 0). The mafic rocks of the Suomenniemi complex have more juvenile (mantle-like) isotope compositions (ε_{Ndi} of -1 to +1; $\delta^{18}O$-in-zircon of 5.5‰; ε_{Hfi} of +4).

In view of the fact that point-specific errors on the $^{206}Pb/^{238}U$ and $^{207}Pb/^{235}U$ ratios measured on zircon fractions from the granites and silicic dike rocks of the Suomenniemi complex were not considered by Vaasjoki et al. (1991), we have re-examined the previous data in search of a better conception of the emplacement age of the granites of the Suomenniemi batholith and the quartz-feldspar porphyry dikes that cut both the granites of the batholith and the surrounding Svecofennian bedrock (Fig. 1). We also present new U-Pb zircon secondary ion microprobe data for one of the granite samples analyzed previously by Vaasjoki et al. (1991), as the conventional zircon fractions from this granite showed abnormally large scatter and, consequently, increased uncertainty on the emplacement age and potential consanguinity of the granite series of the batholith. Using the U-Pb emplacement age of the granites of the Suomenniemi batholith, we apply the refined decay constant

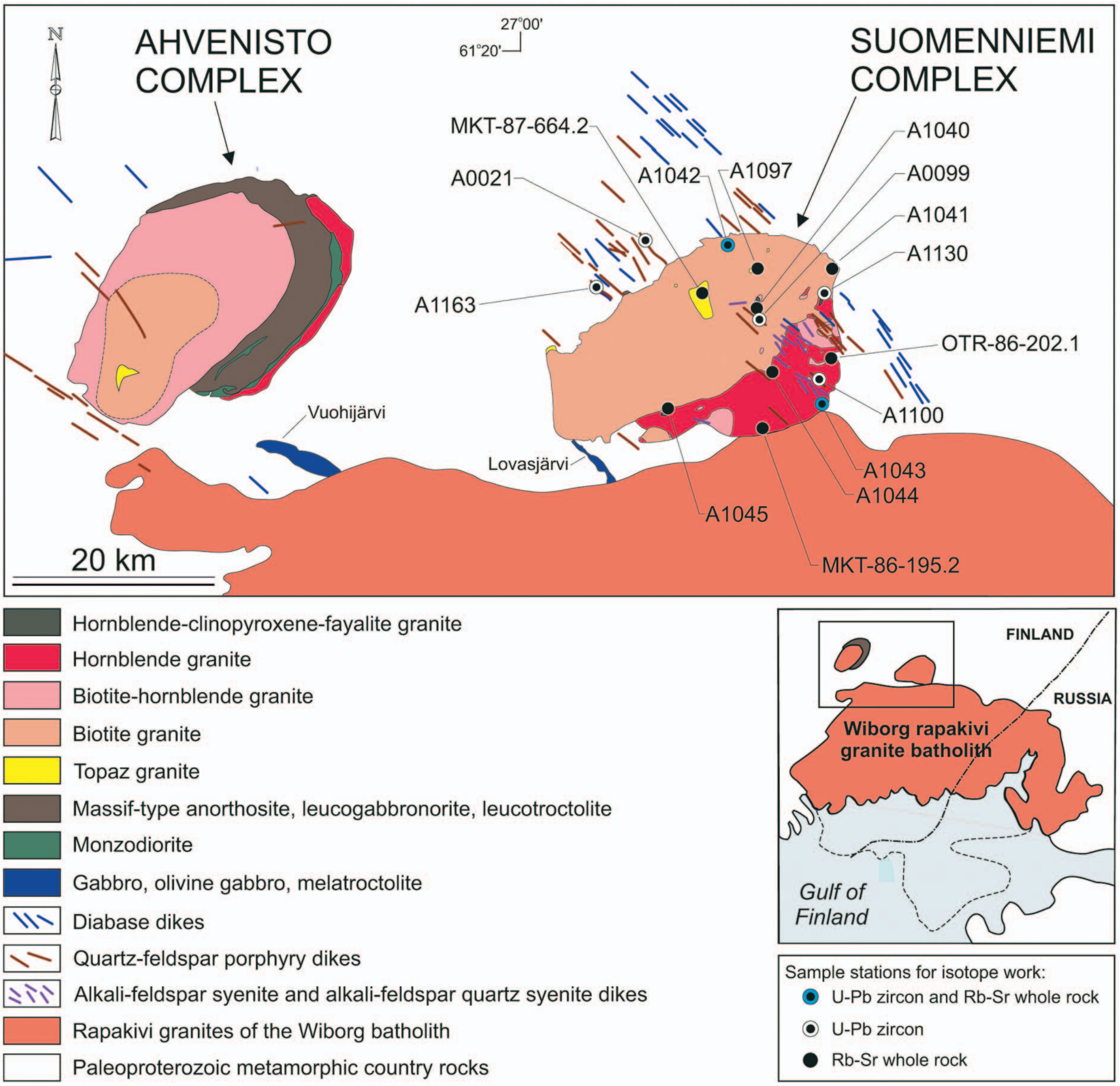

Fig. 1. Geological map of the northern flank of the Wiborg rapakivi granite batholith, showing the lithologic assemblages of two prominent ~1.64 Ga satellite complexes, Suomenniemi and Ahvenisto. Two gabbroic intrusions, Vuohijärvi and Lovasjärvi, presumably related to the diabase dikes, are also shown. For the Suomenniemi complex, location of the isotope samples discussed in this paper are shown as delivered in the station legend. Inset shows map area relative to the Wiborg batholith (dashed line indicates the extent of the batholith under the Gulf of Finland). Modified from Lehijärvi & Tyrväinen (1969), Alviola (1981), Siivola (1987), Rämö (1991, 1999) and Rämö et al. (2014).

of ^{87}Rb (Nebel et al., 2011; Rotenberg et al., 2012) to re-evaluate the whole-rock Rb-Sr data set published earlier on the granite series of the Suomenniemi batholith (Rämö, 1991). It appears that (1) the main granite series of the Suomenniemi complex crystallized at 1644±4 Ma and is measurably older than the quartz-feldspar porphyry dikes (1634±4 Ma); (2) the granite series of the Suomenniemi batholith cooled quite rapidly to the closure temperature of the Rb-Sr isotope system; (3) the measured whole-rock Rb-Sr compositions date the emplacement of the granites within the analytical error involved, and thus (4) the implied $^{87}Sr/^{86}Sr_i$ of 0.7062±0.0024 is a valid (yet only fair) estimate of the initial isotope composition of the granite series. This initial ratio points to a major Paleoproterozoic (Svecofennian) crustal component in the magma from which the granite series crystallized.

2. The silicic rocks of the Suomenniemi complex

The silicic rocks of the Suomenniemi complex include the main granite series and cross-cutting quartz-feldspar porphyry dikes (Rämö, 1991). The granites constitute the Suomenniemi batholith and comprise four main types (Fig. 1): hornblende granite, biotite-hornblende granite, biotite granite, and topaz granite. In addition, there is a volumetrically minor intrusive phase of hornblende-clinopyroxene-fayalite granite that is chilled against and sharply cuts the hornblende granite and biotite-hornblende granite in the eastern and southern parts of the batholith (Fig. 1). The four main granite types form a fractionation series that ranges from low-SiO_2, metaluminous granites to high-SiO_2, marginally peraluminous granites, as illustrated in a SiO_2 vs. A/CNK diagram in Fig. 2. The highly fractionated topaz granites in the northern part of the batholith have, in general, anomalously high Rb and low Sr and Zr concentrations (Table 1; see also Haapala, 1997 and Lukkari, 2007). At a given SiO_2 value, the A/CNK value of the granites varies considerably, probably because of the effect of feldspar accumulation, with high relative Al (high A/CNK) characterizing the samples with excess feldspar (Fig. 2). Rämö (1991) related this granite fractionation series to a common, relatively silicic parental magma.

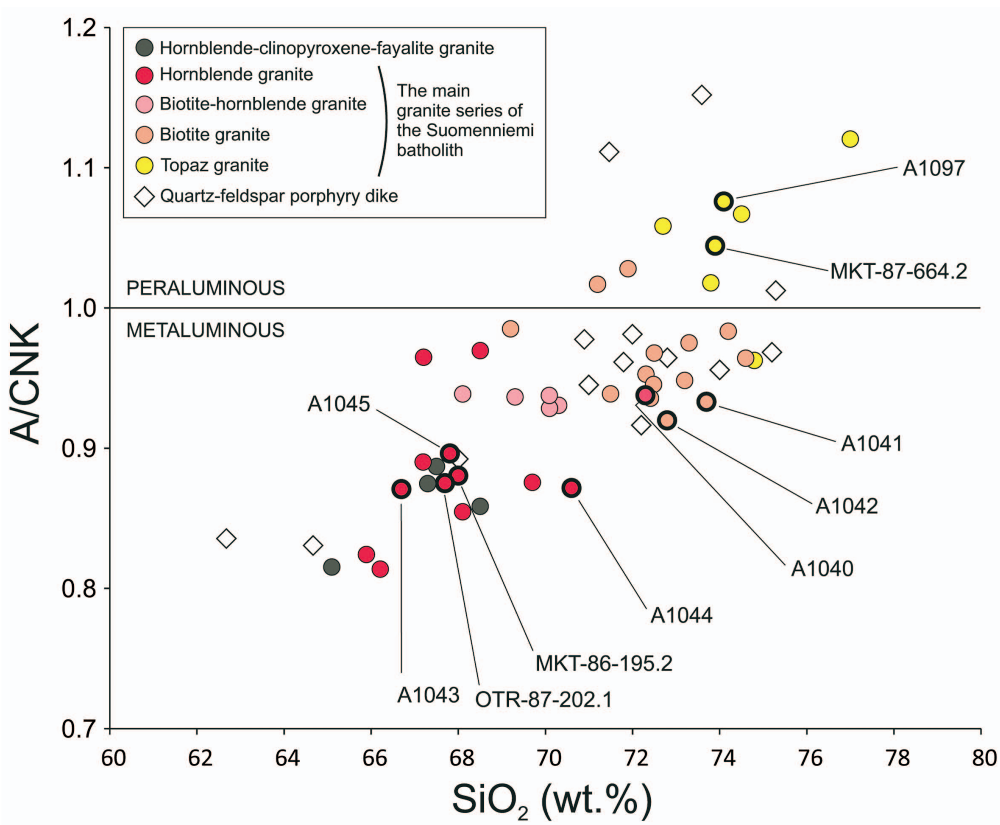

Fig. 2. SiO_2 vs. A/CNK (molar $Al_2O_3/(CaO+Na_2O+K_2O)$) diagram showing the composition of the granites and quartz-feldspar porphyry dikes of the Suomenniemi complex. A/CNK=1 is the divide between metaluminous and peraluminous fields. The ten samples analyzed for whole-rock Rb-Sr isotopes from the main granite series of the Suomenniemi batholith are indicated. Data from Rämö (1991).

Table 1. Whole-rock geochemical parameters, Rb-Sr isotope data, and initial ^{87}Sr-^{86}Sr ratios for the main granite series of the Suomenniemi batholith, southeastern Finland

Sample [1]	SiO_2 (wt.%)	A/CNK [2]	Zr (ppm)	Rb [3] (ppm)	Sr [3] (ppm)	$^{87}Rb/^{86}Sr$ [4]	$^{87}Sr/^{86}Sr$ [5] (at present)	$^{87}Sr/^{86}Sr$ [6, 9] (at 1644 Ma with $\lambda_{87} = 1.42*10^{-11}a^{-1}$)	$^{87}Sr/^{86}Sr$ [7, 9] (at 1644 Ma with $\lambda_{87} = 1.3968*10^{-11}a^{-1}$)	$^{87}Sr/^{86}Sr$ [8, 9] (at 1644 Ma with $\lambda_{87} = 1.393*10^{-11}a^{-1}$)
Hornblende granite										
OTR-87-202.1	67.7	0.875	594	144.9	190.1	2.217	0.760419 ± 27	0.70806 ± 0.00033	0.70892 ± 0.00033	0.70906 ± 0.00033
MKT-86-195.2	68.0	0.880	637	182.0	156.2	3.398	0.786347 ± 24	0.70609 ± 0.00047	0.70742 ± 0.00047	0.70763 ± 0.00046
A1043	66.7	0.872	595	177.2	169.1	3.052	0.777363 ± 16	0.70528 ± 0.00043	0.70647 ± 0.00042	0.70666 ± 0.00042
A1044	70.6	0.871	840	238.6	78.75	8.942	0.913227 ± 15	0.70202 ± 0.00114	0.70551 ± 0.00112	0.70608 ± 0.00112
A1045	67.8	0.896	488	255.1	151.1	4.935	0.818894 ± 15	0.70233 ± 0.00066	0.70426 ± 0.00065	0.70457 ± 0.00065
Biotite-hornblende granite										
A1040	72.3	0.938	576	229.0	98.35	6.837	0.862640 ± 10	0.70115 ± 0.00089	0.70382 ± 0.00087	0.70426 ± 0.00087
Biotite granite										
A1041	73.7	0.933	435	351.0	58.35	18.10	1.119189 ± 18	0.69168 ± 0.00224	0.69874 ± 0.00220	0.69990 ± 0.00220
A1042	72.8	0.920	368	321.6	65.93	14.57	1.039237 ± 15	0.69510 ± 0.00181	0.70079 ± 0.00179	0.70172 ± 0.00178
Topaz granite										
MKT-87-664.2	73.9	1.044	123	683.0	19.10	134.9	3.82024 ± 6	0.63398 ± 0.01628	0.68664 ± 0.01601	0.69526 ± 0.01598
A1097	74.1	1.076	39	695.9	9.06	442.4	10.84869 ± 24	0.39946 ± 0.05323	0.57215 ± 0.05236	0.60042 ± 0.05222

Note: Elemental geochemical data from Rämö (1991), isotope-dilution data from Rämö (1999)

1) For sample coordinates, see Table 1 in Rämö (1999)
2) Molecular $Al_2O_3/(CaO+Na_2O+K_2O)$
3) Measured by isotope dilution
4) Atomic ratio; estimated error is better than 0.5%
5) Normalized to $^{86}Sr/^{88}Sr = 0.1194$. Within-run precision expressed as $2\sigma_m$ in the last significant digits; external error is 0.009% (2σ)
6) Initial ratios calculated at 1644 Ma using the ^{87}Rb decay constant $1.42*10^{-11}a^{-1}$ (Steiger and Jäger, 1977)
7) Initial ratios calculated at 1644 Ma using the ^{87}Rb decay constant $1.3968*10^{-11}a^{-1}$ (Rotenberg et al., 2012)
8) Initial ratios calculated at 1644 Ma using the ^{87}Rb decay constant $1.393*10^{-11}a^{-1}$ (Nebel et al., 2011)
9) External errors in $^{87}Rb/^{86}Sr$ and $^{87}Sr/^{86}Sr$ included

Overall, the main granite series of the Suomenniemi batholith probably reflects fractionation of mainly alkali feldspar, quartz, and a subaluminous mafic silicate from a primary magma that straddled the metaluminosity-peraluminosity boundary (cf. Zen, 1986; Shearer & Robinson, 1988; Emslie, 1991). At the current level of exposure, the most primitive (low-SiO_2) granites are found in the southern and the most evolved (high-SiO_2) granites in the northern part of the batholith (Fig. 1). According to Vaasjoki et al. (1991), the marginal parts of the Wiborg batholith just south of the Suomenniemi batholith are ~10 Ma younger than the granites of the Suomenniemi batholith (see also Rämö et al., 2014), and the distribution of the granite types in the Suomenniemi batholith has been claimed to result from north-northeast tilting caused by the emplacement of the Wiborg batholith (Rämö, 1991).

About 40 quartz-feldspar porphyry dikes are found within the Suomenniemi complex (Rämö, 1991). The dikes strike northwest, dip vertically, are commonly 5 to 20 m wide, and cut both the granites of the Suomenniemi batholith and its Svecofennian country rocks (Fig. 1). The dikes have often dark and aphanitic (originally sometimes vitrophyric) margins, whereas the central parts are composed of alkali feldspar (rounded or angular), quartz, and plagioclase phenocrysts and polycrystalline hornblende-biotite aggregates after mafic pyrogenic phenocrysts, set in a fine- to medium-grained granitic groundmass. These dikes obviously represent a later phase of rapakivi granite magma emplaced along a prevailing northwest-striking fracture system, subsequent to the solidification of the granites of the Suomenniemi batholith (Rämö, 1991). Geochemically, the quartz-feldspar porphyry dikes conform to the granites of the batholith (Fig. 2).

3. Previous work and samples

Previously, seven samples have been collected for U-Pb zircon chronology from the granites and quartz-feldspar porphyry dikes of the Suomenniemi complex. Kouvo (1958) sampled two quartz-feldspar porphyry dikes – the Mentula dike (sample A0021), which cuts the Svecofennian bedrock just north of the Suomenniemi batholith, and the Kiesilä dike (sample A0099), which cuts the main granite series in the central part of the batholith (Fig. 1). Vaasjoki et al. (1991) collected three granite samples, the Pohjalampi hornblende granite (sample A1043) from the southeastern flank of the batholith, the Uiruvuori biotite granite (sample A1042) from the northern part of the batholith, and the Sikolampi hornblende-clinopyroxene-fayalite granite (A1130) from the main body of fayalite-bearing granites; the hornblende-clinopyroxene-fayalite granite cuts the hornblende granites and biotite-hornblende granites of the main granite series of the batholith (Fig. 1). The results of the U-Pb zircon analyses on these three granite samples were summarized by Vaasjoki et al. (1991), with upper intercept ages being 1639±6 Ma, 1641±2 Ma, and 1636±23 Ma for the Uiruvuori, Pohjalampi, and Sikolampi granites, respectively. Vaasjoki et al. (1991) also collected two additional samples from quartz-feldspar porphyry dikes, the Nikkari dike (sample A1100), which is strongly chilled against the hornblende granite in the southeastern part of the Suomenniemi batholith, and the Viitalampi dike (sample A1163), which cuts the Svecofennian metamorphic country rocks northwest of the batholith (Fig. 1) and is commingled with diabase. Vaasjoki et al. (1991) reported upper intercept ages of 1638±32 Ma, 1639±9 Ma, 1635±2 Ma, and 1636±16 Ma for the Mentula, Kiesilä, Nikkari, and Viitalampi dikes, respectively.

Of the main granite series of the Suomenniemi batholith, ten samples have been analyzed for whole-rock Rb-Sr isotopes (Fig. 1; Rämö, 1999). In addition to the Uiruvuori and Pohjalampi granites analyzed for zircon U-Pb, these comprise four hornblende granites (OTR-87-202.1, MKT-86-195.2, A1044, A1945), a biotite-hornblende granite (A1045), a biotite granite (A1042) and two topaz granites (MKT-87-664.2, A1097). The ten samples fall on an errorchron with a MSWD (Mean Square of Weighted Deviates) of 28.9 and $^{87}Sr/^{86}Sr_i$ of 0.7066± 0.0023. An age of 1600±7 Ma can be calculated from the least-squares fit of the Rb-Sr isotope data on these samples (cf. Rämö, 1999). This age has a relatively small error and is younger than the ~1640-Ma U-Pb zircon age reported by Vaasjoki et al. (1991).

4. Analytical methods and procedures

4.1. Discordia fits of U-Pb zircon data points

For age determination based on zircon, conventional multi-grain isotope dilution U-Pb data are fitted to a least-squares regression line in the $^{207}Pb/^{235}U$ vs. $^{206}Pb/^{238}U$ space (York, 1969). The reliability of the fit is dependent on the precision and accuracy of the analytical results on individual multi-grain zircon fractions and may vary depending on, among other things, the relative amount of radiogenic Pb in the analyzed fraction and resultant variation in the precision of the mass spectrometric measurements of U and Pb. The data elaborations by Vaasjoki et al. (1991) were based on age calculations utilizing a common error of the Pb/U ratios (±0.8%) as well as a common error correlation of the $^{207}Pb/^{235}U$ and $^{206}Pb/^{238}U$ ratios (90%). We have recalculated the U-Pb zircon data on the four granites of the Suomenniemi batholith using external errors and error correlations of individual zircon fractions in search of enhanced accuracy.

4.2. U-Pb zircon secondary ion mass spectrometry

For in situ U-Pb work on the Uiruvuori biotite granite, zircon grains from heavy mineral fractions, recovered from sample A1042 by Vaasjoki et al. (1991), were examined for internal textures using SEM imaging. Grains chosen for secondary ion microprobe analysis were mounted in epoxy, polished, and coated with gold. The ion microprobe U-Pb analyses were performed using the Nordic Cameca IMS 1270 instrument at the Swedish Museum of Natural History, Stockholm, Sweden (the NordSIM facility). The used spot diameter for the 4nA primary negative O_2 ion beam was ~30 µm and oxygen flooding in the sample chamber was used to increase the transmission of lead. The mass resolution (M/ΔM) was approximately 5600 (10%). Four counting blocks, each including three cycles of the Zr, Pb, Th, and U species were measured for every spot. The raw data were calibrated against the zircon standard 91500 (Wiedenbeck et al., 1995) and corrected for background (204.2) and age-related common lead (Stacey and Kramers, 1975). A detailed description of the analytical process is available in Whitehouse et al. (1999) (see also Whitehouse & Kamber, 2005). Plotting of the U-Pb isotope data, fitting of the discordia lines, and calculating the ages were performed using the Isoplot/Ex 3 program (Ludwig, 2003). Age errors were calculated at 2σ and decay constants errors were ignored. Data-point error ellipses in the illustrations are shown at 2σ.

4.3. Recalculation of whole-rock Rb-Sr isotopic ages

Applicability of isotopic dating methods based on radioactive decay is profoundly dependent on the accuracy of the decay constant λ. For the Rb-Sr isotope method, the value of λ_{Rb} ($1.42*10^{-11}a^{-1}$) was approved by the Subcommission on Geochronology of the International Union of Geological Sciences in 1977 (Steiger and Jäger, 1977). This value of λ_{Rb} has not, however, gained universal acceptance (e.g., Begemann et al., 2001). New endeavors set out to improve the accurracy of λ_{Rb} include direct β^- counting (Kossert, 2003), geological age-comparison using a better-known decay system (Amelin & Zaitsev, 2002; Nebel et al., 2011), and ingrowth measurement of daughter isotope accumulated over a laboratory time scale (e.g., Rotenberg et al., 2012). These studies indicate that compared to the value recommended by Steiger and Jäger (1977), the potentially more applicable value of λ_{Rb} is lower, probably on the order of $1.393*10^{-11}a^{-1}$ to $1.397*10^{-11}a^{-1}$. This difference implies that the Rb-Sr isochron ages determined using the approved λ_{Rb} are 1-2% too young. We have reassessed the whole-rock Rb-Sr isotope data on the main granite series of the Suomenniemi complex using the isotope ratios determined by Rämö (1999) and the new, lower values of λ_{Rb}.

5. Results

5.1. U-Pb zircon geochronology

U-Pb zircon multi-grain isotope data on the Uiruvuori (A1042) biotite granite, the Pohjalampi hornblende granite (A1043), the Sikolampi hornblende-augite-fayalite granite (A1130), and four quartz-feldspar porphyry dikes (A0021 Mentula, A0099 Kiesilä, A1100 Nikkari, and A1163 Viitalampi) are shown in the appended table (Table A1) and in concordia diagrams in Fig. 3. U-Pb zircon secondary ion microprobe data on eight spots from six grains of the Uiruvuori biotite granite A1042 are shown in Table 2 and in a concordia diagram in Fig. 3.

Uiruvuori (A1042) biotite granite

The five zircon fractions (A through E; Table A1) analyzed by Vaasjoki et al. (1991) from the Uiruvuori biotite granite sample taken from a quarry on the northern flank of the batholith (Fig. 1) define a discordia line with concordia intercepts at 1643±19 Ma and 118±121 Ma and a MSWD of 4.9 (Fig. 3a). The four most concordant fractions (A through D) fall on a discordia with an upper intercept age of 1640±9 Ma, a lower intercept age of 83±56 Ma, and a MSWD of 1.2. This upper intercept age is compatible with the $^{207}Pb/^{206}Pb$ age of the most concordant fraction A1042-C (1636±7 Ma) and is the preferred crystallization age of the Uiruvuori biotite granite.

The relatively large error of ±9 Ma in the upper intercept age of the Uiruvuori biotite granite was scrutinized by analyzing eight *in situ* U-Pb spots from six zircon grains using the NordSIM secondary ion microprobe. Examples of the analyzed grains are shown in Fig. 4, analytical data (Table 2) in Fig. 3b, and a $^{207}Pb/^{206}Pb$ age plot in Fig. 5. Zircon grains from the Uiruvuori biotite granite are prismatic and rich in inclusions. Two textural types can be recognized – those grains that have heavy (in BSE

Table 2. Secondary ion microprobe U-Pb zircon data for the Uiruvuori biotite granite (sample A1042) of the main granite series of the Suomenniemi rapakivi granite batholith

Spot no.	Analyzed zircon domain	Ages (Ma) [1] $^{207}Pb/^{206}Pb$	$^{207}Pb/^{235}U$	$^{206}Pb/^{238}U$	Calibrated ratios [2] $^{207}Pb/^{206}Pb$	$^{207}Pb/^{235}U$	$^{206}Pb/^{238}U$	ρ [3]	Disc. % [4]	U (ppm)	Th (ppm)	Pb (ppm)	Th/U calc.	Th/U meas.	$^{206}Pb/^{204}Pb$ meas.
n752-12a	ho-outer part	1641 ± 6	1596 ± 12	1562 ± 21	0.1009 (0.30)	3.814 (1.53)	0.2741 (1.50)	0.98	-2.3	581	259	195	0.40	0.45	1.68E+0.5
n752-33a	ho-heavy inner	1625 ± 4	1622 ± 12	1620 ± 22	0.1000 (0.24)	3.941 (1.52)	0.2858 (1.50)	0.99		1000	554	364	0.60	0.55	7.79E+0.4
n752-33b	zo-light outer	1620 ± 7	1615 ± 13	1612 ± 21	0.0998 (0.37)	3.909 (1.55)	0.2841 (1.50)	0.97		404	174	142	0.45	0.43	7.64E+0.4
n752-35a	ho-heavy inner	1623 ± 5	1645 ± 12	1662 ± 22	0.0999 (0.25)	4.053 (1.52)	0.2942 (1.50)	0.99		3203	2796	1282	0.92	0.87	2.04E+0.5
n752-36a	ho-heavy inner	1617 ± 4	1597 ± 12	1583 ± 21	0.0996 (0.23)	3.822 (1.51)	0.2783 (1.50)	0.99		1964	1629	765	1.00	0.83	6.89E+0.4
n752-36b	zo-light outer	1637 ± 5	1559 ± 12	1502 ± 20	0.1007 (0.27)	3.641 (1.52)	0.2623 (1.50)	0.98	-6.2	970	340	308	0.35	0.35	1.92E+0.4
n752-39a	ho-heavy inner	1641 ± 5	1624 ± 13	1612 ± 22	0.1009 (0.29)	3.951 (1.60)	0.2840 (1.57)	0.98		2011	1866	810	1.07	0.93	7.01E+0.4
n752-40a	zo-heavy inner	1616 ± 8	1580 ± 13	1552 ± 21	0.0996 (0.45)	3.738 (1.57)	0.2723 (1.50)	0.96	-0.8	764	261	253	0.38	0.34	8.99E+0.3

Note: Analyses performed using the NordSIM Cameca IMS 1270 secondary ion microprobe at the Swedish Museum of Natural History, Stockholm, Sweden. Common Pb correction according to the Pb isotope composition of galena from the Suursaari Island (Vaasjoki, 1977): $^{206}Pb/^{204}Pb$ = 15.91, $^{207}Pb/^{204}Pb$ = 15.37, $^{208}Pb/^{204}Pb$ = 35.38. Key to abbreviations: ho-homogeneous, zo-zoned.

[1] Errors denoted at the 1σ level.
[2] Numbers in parentheses are 1σ errors (in percent) of calibrated ratios.
[3] $^{207}Pb/^{235}U$ – $^{206}Pb/^{238}U$ error correlation.
[4] Degree of discordance, calculated at the closest 2σ limit. Blank if concordant.

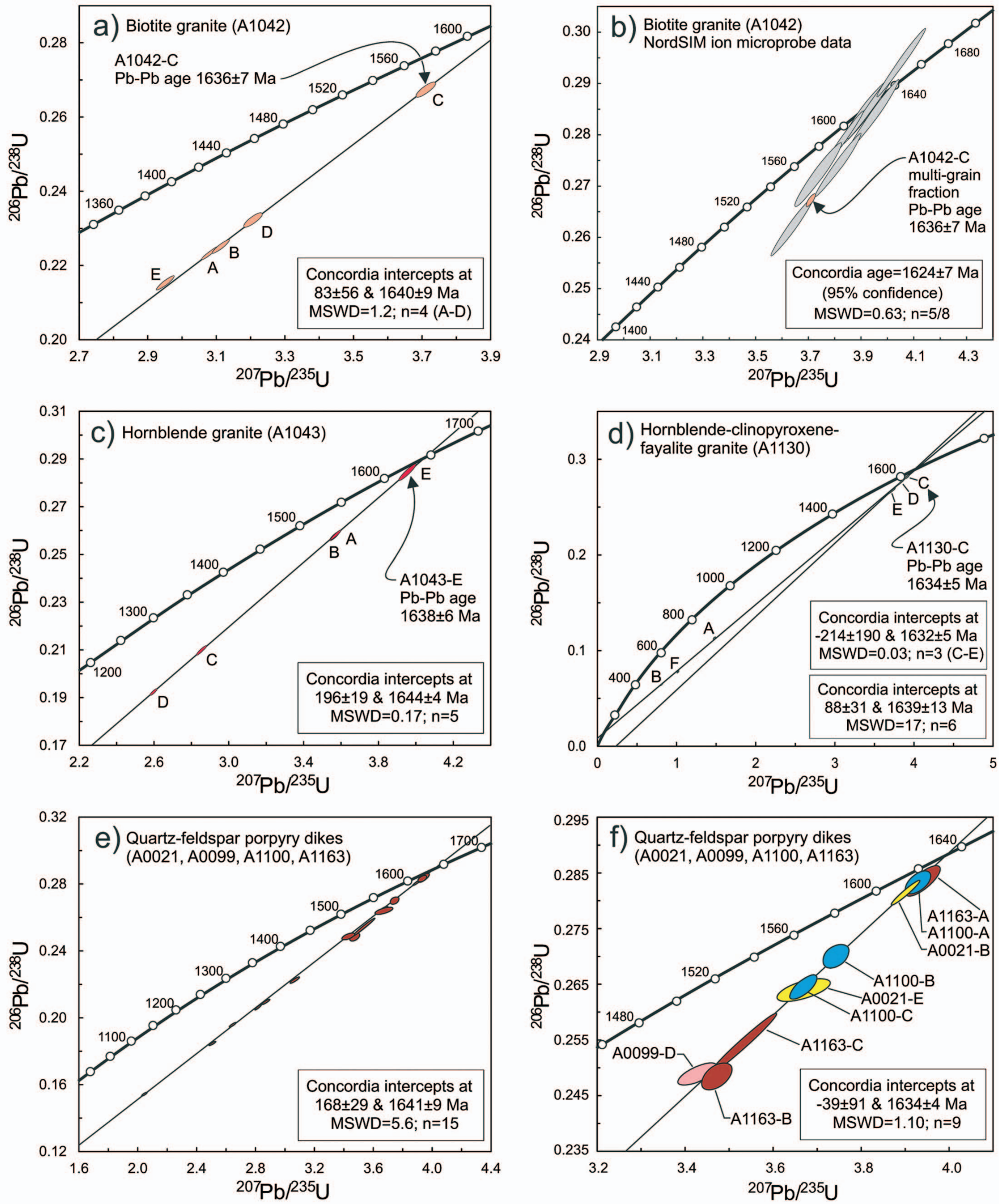

Fig. 3. U-Pb concordia diagrams showing the results of zircon U-Pb analyses (Table A1) on three granites and four quartz-feldspar porphyry dikes from the Suomenniemi complex. a) Multi-grain data on the Uiruvuori (A1042) biotite granite. b) Secondary ion microprobe data on the Uiruvuori granite. c) Multi-grain data on the Pohjalampi hornblende granite (A1043). d) Multi-grain data on the Sikolampi hornblende-clinopyroxene-fayalite granite (A1130). e) & f) Multi-grain data on the Mentula (A0021), Kiesilä (A0099), Nikkari (A1100), and Viitalampi (A1163) quartz-feldspar porphyry dikes; in f), varying colors are used for illustrative purposes. Error ellipses are at the 2σ level.

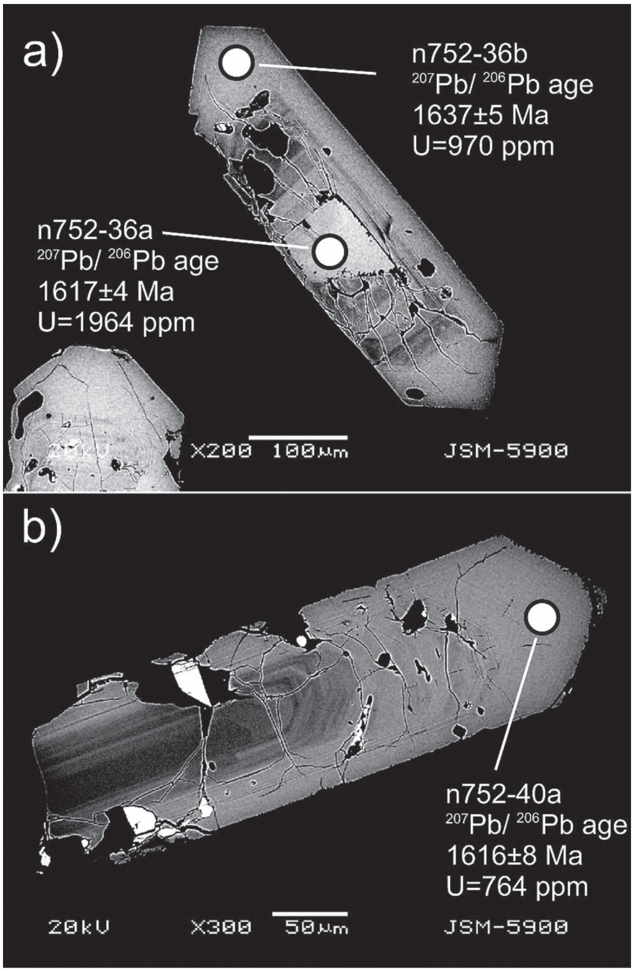

Fig. 4. Back-scattered electron images of two of the five zircon crystals analyzed by secondary-ion microprobe for their U-Pb isotope composition from the Uiruvuori biotite granite (A1042). a) Grain n752-36 that shows distinct central and rim parts with grossly different U values. b) Grain n752-40 that shows pervasive magmatic zoning. The white circles indicate secondary ion microprobe spot locations (Table 2).

images bright) central parts and light (in BSE images dull) overgrowths (Fig. 4a) and those grains that are pervasively zoned and light (in BSE images dull) (Fig. 4b). The concordia age of the five concordant U-Pb compositions (Fig 3b; see also Table 2) is 1624±7 Ma (MSWD=0.63).

Figure 5 shows a weighted average ^{207}Pb/^{206}Pb age plot of the eight spots analyzed from the Uiruvuori biotite granite. For all eight spots, the weighted average ^{207}Pb/^{206}Pb age is 1627±9 Ma (MSWD=3.9). The data, however, seem to fall into two groups: the three spots with the highest ^{207}Pb/^{206}Pb ages average at 1639.5±6.0 Ma (MSWD=0.20) and the five spots with the lowest ^{207}Pb/^{206}Pb ages at 1620.9±4.4 Ma (MSWD=0.64). The older age conforms to the multigrain upper intercept age of 1640±9 Ma of the sample (Fig. 3a). The two average ages, 1640±6 Ma and 1621±5 Ma, are probably real. A possible reason for this age difference is illustrated by the analyzed grain number n752-36 (Table 2) that has a bright interior and dull outer part (Fig. 4a). The heavy central part of the crystal is very high in U (1964 ppm) and the light rim is relatively low in U (970 ppm). ^{207}Pb/^{206}Pb dates of the center and rim are 1617±4 Ma and 1637±5 Ma, respectively. The dates of the center and rim parts of this zircon crystal are thus probably measurably different. This may reflect the possibility that the U-Pb system of high-U zircon domains may remain open longer than that of low-U domains and hence register a younger age. The scatter shown by the multi-grain fractions (Fig. 3a) could thus be, at least in part, a reflection of highly varying U content in various structural parts of zircon grains. Further causes for the heterogeneity are, however, implied by the pervasively zoned, more homogeneous crystal n752-40 (Fig. 4b), which has a young rim with a ^{207}Pb/^{206}Pb age of 1616±8 Ma and a relatively low U value (764 ppm).

Pohjalampi hornblende granite (A1043)

For the Pohjalampi hornblende granite on the southeastern flank of the Suomenniemi batholith (Fig. 1), Vaasjoki et al. (1991) published the five-fraction upper and lower intercept ages of 1641±2 Ma and 191±9 Ma, respectively. Point-specific errors on Pb/U considered, these five zircon fractions define a good discordia (MSWD=0.17) with concordia intercepts at 1644±4 Ma and 196±19 Ma (Fig. 3c). The ^{207}Pb/^{206}Pb age of the most concordant fraction A1043-E is 1638±6 Ma. The upper intercept age, 1644±4 Ma, is considered an accurate and relatively precise estimate of the crystallization age of the Pohjalampi hornblende granite.

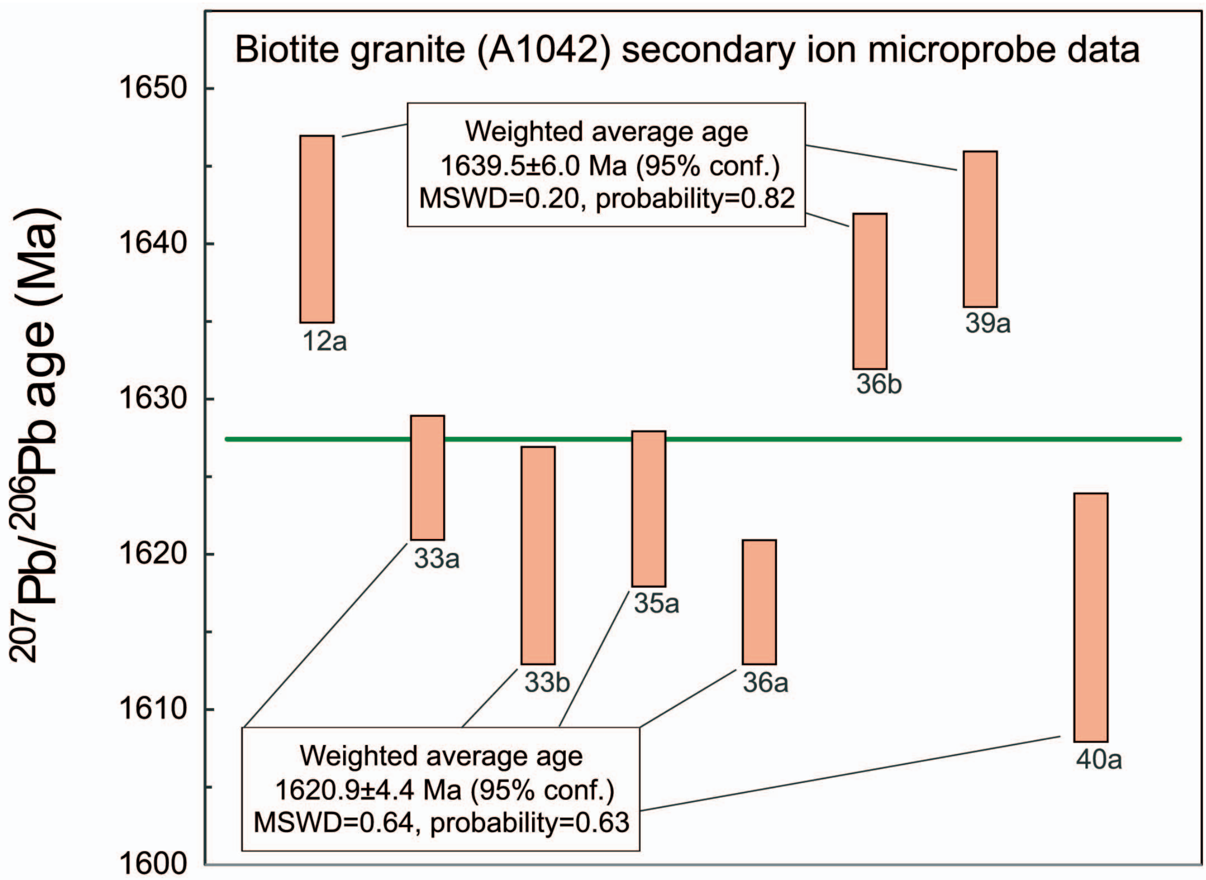

Fig. 5. Weighted average plot of the $^{207}Pb/^{206}Pb$ ages of the eight zircon spots (Table 2, as labeled) analyzed by secondary ion microprobe for their U-Pb isotope composition from the Uiruvuori biotite granite (A1042). Combined, the eight samples deliver a weighted average age of 1627±9 Ma (MSWD=3.9). The data can be divided into two groups with distinct weighted average ages (1640±6 Ma and 1621±5 Ma).

Sikolampi hornblende-clinopyroxene-fayalite granite (A1130)

The six multi-grain fractions (Table A1) originally analyzed by Vaasjoki et al. (1991) from the Sikolampi hornblende-clinopyroxene-fayalite granite, which cuts a hornblende granite in the eastern part of the batholith (Fig. 1), fall into two categories: three rather concordant and three strongly discordant fractions (Table A1; Fig. 3d). Altogether, they define a discordia with intercepts of 1639±13 Ma and 88±31 Ma and a MSWD of 17 (Fig. 3c). The three most concordant fractions (C through E) define an upper intercept age of 1632±5 Ma with a MSWD of 0.03. In view of the 1634±5 Ma $^{207}Pb/^{206}Pb$ age of the most concordant fraction A1130-C, the three-point upper intercept age is probably a valid estimate of the crystallization age of the Sikolampi granite.

Quartz-feldspar porphyry dikes (A0021, A0099, A1100, A1163)

The U-Pb data reported for the 15 multi-grain fractions from these four dikes by Vaasjoki et al. (1991) (Table A1) define a discordia with intercepts at 1641±9 Ma and 168±29 Ma and a MSWD of 5.6 (Table A1; Fig. 3e). Nine of the most concordant fractions imply intercept ages of 1634±4 Ma and -39±91 Ma (Fig. 3f). This nine-point fit is internally consistent (MSWD=1.10) and compatible with the $^{207}Pb/^{206}Pb$ ages of the three most concordant fractions (A0021-B 1633±4 Ma; A1100-A 1635±11 Ma; A1163-A 1638±10 Ma) and is considered as the emplacement age of these dikes. Two of the dikes (A0099, A1100) cut the main granite series of the batholith and two of them (A0021, A1163) the Svecofennian country rocks of the batholith and probably belong to a single magmatic event that clearly postdates the emplacement of the main granite series of the Suomenniemi batholith.

5.2. Rb-Sr whole-rock geochronology

Rb-Sr isotopic data for the ten granite samples from the Suomenniemi batholith from Rämö (1999) are shown in Table 1 and in a Rb-Sr isochron diagram in Fig. 6. In the $^{87}Rb/^{86}Sr$ vs. $^{87}Sr/^{86}Sr$ space, the data define a regression line with the following equation:

$$^{87}Sr/^{86}Sr = (0.022980 \pm 0.000097) * {}^{87}Rb/^{86}Sr + 0.7066 \pm 0.0023 \quad (1)$$

The time t associated with this fit, representing the time in the past when the analyzed samples had the same, initial, $^{87}Sr/^{86}Sr$ ratio, is calculated from the slope m (in this case 0.022980±0.000097) and λ_{87} (the decay constant of ^{87}Rb) of the line as

$$t = \ln(m+1)/\lambda_{87} \quad (2)$$

Using the official λ_{87} value of Steiger & Jäger (1977), an age of 1600±7 Ma is calculated from this fit. Using the λ_{87} values of Nebel et al. (2011) and Rotenberg et al. (2012), ages of 1631±7 Ma and 1627±7 Ma are calculated. If the highest Rb/Sr sample (the Pohjalampi topaz granite A1097; Table 1) is omitted, the slope and the ordinate intercept become 0.023077±0.000141 and 0.7062±0.0024, respectively, with an MSWD of 31. The ages calculated from equation (2) for this fit are 1604±10 Ma (λ_{87} from Steiger & Jäger, 1977), 1635±10 Ma

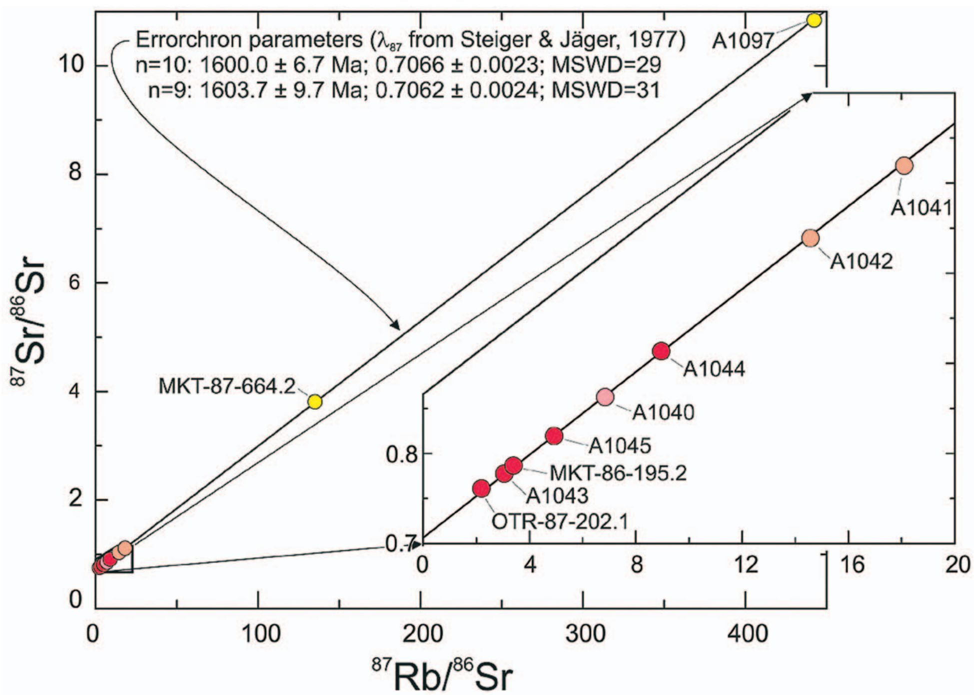

Fig. 6. $^{87}Rb/^{86}Sr$ vs. $^{87}Sr/^{86}Sr$ diagram for the main granite series of the Suomenniemi batholith (Table 1; Rämö, 1991). Two least-squares fits (n = 10, all samples included; n = 9, topaz granite A1097 omitted) are shown with ages calculated using the λ_{87} value of Steiger & Jäger (1977). Color coding of data points as in Fig. 2.

(λ_{87} from Nebel et al., 2011), and 1630±10 Ma (λ_{87} from Rotenberg et al., 2012). Both fits have relatively large MSWD values (29 for n = 10, 31 for n = 9) and are thus errorchrons. They may, however, be used for geochronologic considerations as demonstrated below.

6. Discussion

6.1. Crystallization age of the granites of the Suomenniemi batholith

The main granite series of the Suomenniemi batholith is geochemically relatively coherent (Fig. 2) and probably represents a fractionation array from a common parental magma (cf. Rämö, 1991). Field observations (Rämö, 1991) are compatible with this hypothesis as no discordant contacts between the four main granite types of the batholith have been observed. The U-Pb zircon geochronological data elaborated in this paper comply with this view. The multi-grain upper intercept ages of samples A1043 and A1042 (1644±4 Ma and 1640±9 Ma, respectively) are probably realistic estimates of the crystallization ages of the hornblende granites and biotite granites of the Suomenniemi batholith, considering the external errors involved (Fig. 7). The weighted average $^{207}Pb/^{206}Pb$ zircon age of the older secondary ion microprobe spots from biotite granite A1042 (1640±6 Ma) is compatible with this, as are the $^{207}Pb/^{206}Pb$ ages of the most concordant multi-grain fractions from samples A1042 and A1043 (1636±7 Ma and 1638±6 Ma, respectively: Fig. 3a, b). Overall, and because of the fact that $^{207}Pb/^{206}Pb$ ages of discordant multi-grain zircon fractions represent minimum ages on concordia, the most probable crystallization ages of the hornblende and biotite granites of the Suomenniemi batholith are set by the isotope-dilution upper intercept and secondary ion weighted average ages (Fig. 7). These data imply that the biotite granites and the hornblende granites are probably coeval and that the Pohjalampi hornblende granite, 1644±4 Ma, dates the main hornblende granite-biotite granite volume of the Suomenniemi batholith. The established fractionation series model (Rämö, 1991; see also Fig. 2) of the main granite series further allows the biotite-hornblende granites and the topaz granites to be coeval with the hornblende granites and biotite granites.

The perception thus emerges that the main granite series of the Suomenniemi batholith was crystallized from a single parental magma at 1644±4 Ma. The single sample analyzed from the hornblende-clinopyroxene-fayalite granite, which cuts and is chilled against the hornblende granite of the batholith in the eastern part of it (Fig. 1), has a three-fraction multi-grain zircon upper intercept of 1632±5 Ma and the $^{207}Pb/^{206}Pb$ age of the least discordant fraction is 1635±5 Ma (Figs. 3d, 7). Thus the Sikolampi hornblende-clinopyroxene-fayalite granite may be measurably younger than the main granite series of the Suomenniemi batholith with a possible non-magmatic window of ≤ 1 m.y. (1640-1639 Ma; Fig. 7). Our elaborations imply that there indeed were two different granitic intrusion events that built up the Suomenniemi batholith, as previously proposed (Rämö, 1991).

6.2. Crystallization age of the quartz-feldspar porphyry dikes of the Suomenniemi complex

The quartz-feldspar porphyry dikes that cut sharply across the main granite series of the Suomenniemi batholith and the Svecofennian metamorphic country rocks (medium- to high-grade migmatitic granites) form a geochemically mutually comparable series of silicic rocks with the granites, ranging from low-SiO_2, metaluminous to high-SiO_2, marginally peraluminous compositions (Fig. 2). The multi-grain U-Pb zircon data on the four dikes from both lithologic environments are consistent (Fig. 3e, f) and the pooled age of the four samples define a robust upper intercept age of 1634±4 Ma (Fig. 7). It is probable that the dikes represent a single, volumetrically minor and shallow intrusion event of renewed rapakivi magmatism after the emplacement of the granites of the Suomenniemi batholith. Upon emplacement of the silicic dikes, the granites of the batholith and its host rocks had been cooled and the bedrock around the batholith eroded to a certain extent during an interval of at least two m.y. (1640-1638 Ma). The age of the silicic dikes overlaps with that of the hornblende-clinopyroxene-fayalite granites (Fig. 7) and, in the absence of field observations of their mutual relations, their relative age cannot be fixed. They do, however, represent different environments of emplacement with the quart-feldspar porphyry dikes more clearly postdating the crystallization of the batholith, having been emplaced at a time of more

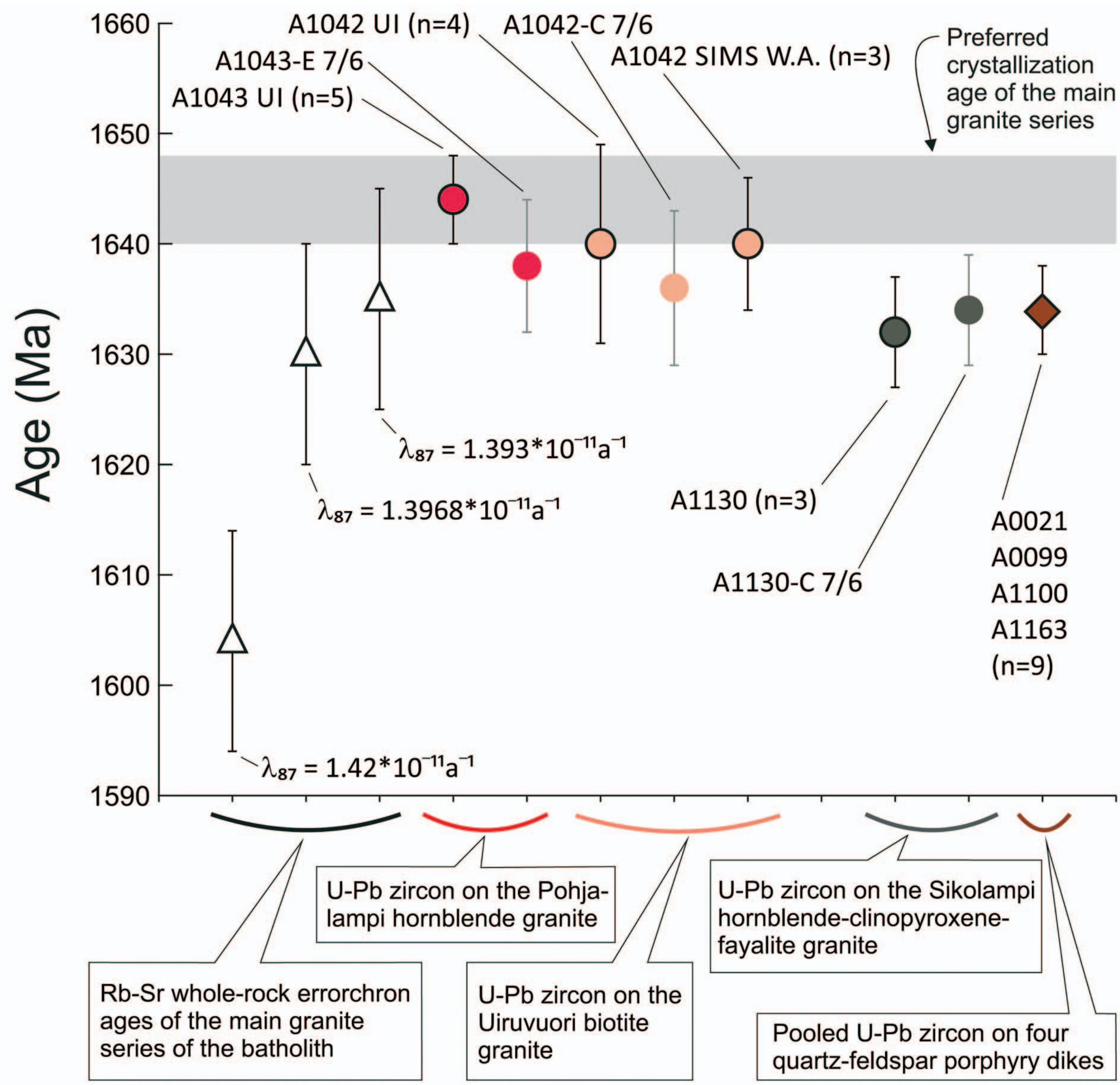

Fig. 7. Comparison of zircon ages of hornblende granite, biotite granite, hornblende-clinopyroxene granite, and quartz-feldspar porphyry dikes and whole-rock Rb-Sr ages of the main granite series of the Suomenniemi complex. Nine-point errorchron (topaz granite A1097 excluded) Rb-Sr ages, calculated using three different values of λ_{87} ($1.42*10^{-11}a^{-1}$, Steiger & Jäger, 1977; $1.393*10^{-11}a^{-1}$, Nebel et al., 2011; $1.3968*10^{-11}a^{-1}$, Rotenberg et al., 2012), are shown. Abbreviations: UI – upper intercept age, 7/6 – multi-grain $^{207}Pb/^{206}Pb$ age, W.A. – weighted average $^{207}Pb/^{206}Pb$ age, SIMS – secondary ion mass spectrometry. Preferred crystallization age (1644±4 Ma) of the main granite series of the Suomenniemi batholith is indicated.

advanced cooling of the main granite series of the batholith.

6.3. Rb-Sr systematics of the main granite series of the Suomenniemi batholith

Adopting the U-Pb zircon emplacement age of the main granite series of the Suomenniemi batholith, 1644±4 Ma, as a piercing point, the Rb-Sr isotope systematics of the granite series may be further scrutinized. In general, Precambrian plutonic igneous systems are prone to have experienced subsolidus events that have affected the magmatic Rb/Sr of the rock suites because of the mobility of Rb and Sr (e.g., Welin et al., 1983). Often the Rb-Sr ratio is increased relative to the magmatic value and the time-corrected initial $^{87}Sr/^{86}Sr$ may thus be unrealistically low. The overcorrection involved may result in calculated "initial" $^{87}Sr/^{86}Sr$ even below the presumed initial $^{87}Sr/^{86}Sr$ of the Solar System at 4.56 Ga ($^{87}Sr/^{86}Sr_i$ = 0.69899 of the Basaltic Achondrite Best Initial, BABI; cf. Faure, 2001).

We calculated the individual $^{87}Sr/^{86}Sr_i$ values for the ten samples originally analyzed from the Suomenniemi granite series by Rämö (1991) using varying λ_{87} values (the official Steiger & Jäger, 1977, value and the lower values published by Nebel et al., 2011 and Rotenberg et al., 2012). The results are shown in Table 1 and in Fig. 8. Some interesting and probably significant patters emerge. Initial ratios calculated using the Steiger & Jäger (1977) value have a very large spread and are grossly deviant from reality because of overcorrection, except for the values calculated for the hornblende granites and biotite-hornblende granite (Fig. 8a, left segment). The topaz granites MKT-87-664.2 and A1097, with the highest present-day $^{87}Rb/^{86}Sr$ (135 and 442) and $^{87}Sr/^{86}Sr$ (3.820 and 10.849), are profusely overcorrected with $^{87}Sr/^{86}Sr_i$ of 0.634±0.016 and 0.399±0.053, respectively (Table 1). For the two lower values of λ_{87}, more internally consistent $^{87}Sr/^{86}Sr_i$ are calculated (Fig. 8a, center and right segments), most of which are nearly compatible within the 2σ external error (Table 1; Fig. 8a, b).

In the light of these calculations, it seems that, using the new λ_{87} values of Nebel et al. (2011) and Rotenberg et al. (2012), all except the very high-Rb/Sr topaz granite A1097 yield single-sample $^{87}Sr/^{86}Sr_i$ values that are relatively compatible with each other (data points within the green dashed fields in Fig. 8a). Hence, the least-squares fit of these nine samples (Fig. 6) may represent a good approximation of the true magmatic equilibrium that governed the crystallization of the main granite series. Thus, the nine-point Rb-Sr errorchron (Fig. 6) may be considered a temporally significant proxy of the solidification stage of the batholith. The relatively large uncertainty involved (MSWD=31), reflected in the shift of the single-sample initial values in Fig. 8, may stem from slight subsolidus modification of Rb/Sr and a slight variation in the initial Sr isotope composition of the granite magma. The effect of the latter was probably minimal, however, because of the homogeneous initial whole-rock Nd and feldspar Pb isotope compositions measured for the main granite series (Rämö, 1991). Errorchron ages of the nine samples (OTR-87-202.1 through MKT-87-664.2 in Table 1), calculated using the new, lower values of λ_{87} (Nebel et al., 2011; Rotenberg et al., 2012), are shown in Fig. 7. These ages are, within the experimental errors involved, compatible with the U-Pb age of the main granite series of the Suomenniemi batholith. Therefore, also the initial $^{87}Sr/^{86}Sr_i$ value calculated from the nine-point fit, 0.7062±0.0024 (Fig. 6), is most probably a magmatic value.

7. Concluding remarks

The Suomenniemi batholith is an important example of A-type granite intrusions with a substantial lithologic variation, which can most likely be ascribed to precipitation from a common parental magma. Our geochronological modeling shows that both the zircon U-Pb and whole-rock Rb-Sr systems of the granites of the main granite series of the batholith register crystallization of the granite series at ~1640 Ma. We prefer the 1644±4 Ma U-Pb zircon age of the main series hornblende granite from the southeastern fringe of the batholith as the best estimate of the emplacement age of the

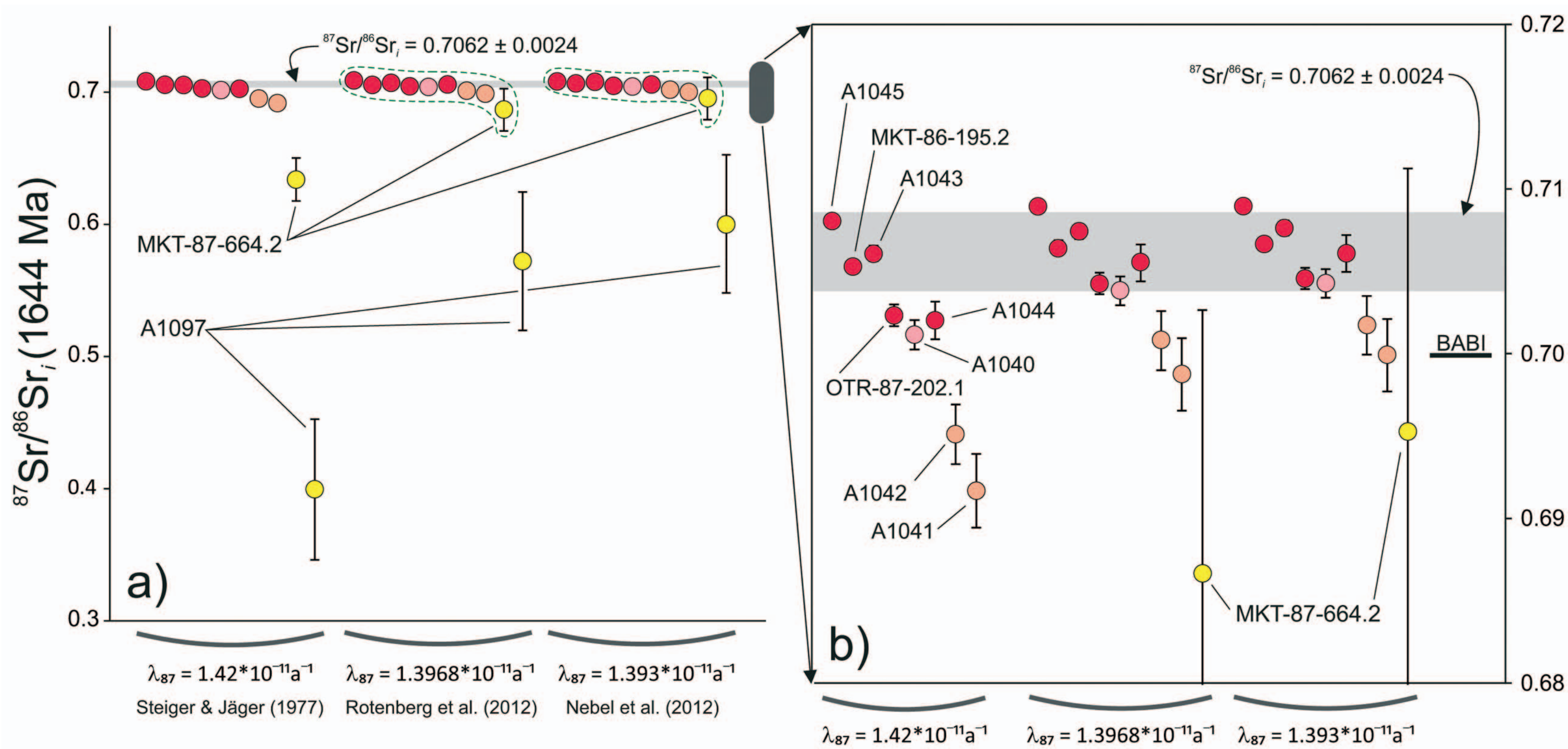

Fig. 8. Single-sample $^{87}Sr/^{86}Sr_i$ values calculated for the ten granite samples (Table 1) of the main granite series of the Suomenniemi batholith using three values of λ_{87} ($1.42*10^{-11}a^{-1}$, Steiger & Jäger, 1977; $1.393*10^{-11}a^{-1}$, Nebel et al., 2011; $1.3968*10^{-11}a^{-1}$, Rotenberg et al., 2012). a) Entire range of calculated $^{87}Sr/^{86}Sr_i$. b) Blow-up of (a) showing the initial ratios of the lower-Rb/Sr samples in detail. $^{87}Sr/^{86}Sr_i$ from the nine-point errorchron fit (0.7062±0.0024) shown in Fig. 6 is also indicated. Calculated initial ratios enclosed by green dashed lines in (a) are reasonably compatible with each other. BABI in (b) is the Basaltic Achodrite Best Initial (cf. Faure, 2001). Error bars on $^{87}Sr/^{86}Sr_i$ are 2σ; in (b) symbol size of the three lowest-Rb/Sr samples (A1045, MKT-86-195.2, A1043) equals the 2σ error on $^{87}Sr/^{86}Sr_i$. Color coding of data points as in Fig. 2.

batholith. The whole-rock Rb-Sr system of the main granite series records, within the external error, the same event and yields a magmatic $^{87}Sr/^{86}Sr_i$ value of 0.7062±0.0024 for the batholith. Compared to the initial value ($^{87}Sr/^{86}Sr_i$ 0.7074±0.0004; Neymark et al., 1994; see also Rämö et al., 1996) of the 1.56 Ga Salmi rapakivi granite batholith in Russian Karelia, showing much more lower ε_{Ndi}, the initial ratio of the Suomenniemi batholith is, at face value, less radiogenic. Compared to the initial values of the rapakivi granite-associated Subjotnian diabase dikes in southern Finland ($^{87}Sr/^{86}Sr_i$ in the 0.7036±0.0003 range; Suominen, 1991), the initial ratio of the Suomenniemi batholith is more radiogenic. These initial Sr isotope compositions probably reflect major material contributions from a mixed Archean-Paleoproterozoic crustal source (Salmi granites), Paleoproterozoic crust (Suomenniemi granites), and Paleoproterozoic sub-continental mantle (Finnish diabase dikes). The preservation of the magmatic Rb-Sr isotope system in the granites of the Suomenniemi batholith implies that the batholith cooled relatively rapidly to the closure temperature of the Rb-Sr system in the granites (probably governed by closure of mica in the high-Rb/Sr samples at ~300-400°C – cf. Dodson, 1973; Del Moro et al., 1982). This must have occurred before the major thermal perturbations that were associated with the emplacement of the Wiborg batholith proper at ~1630 Ma (cf. Rämö et al., 2014; Heinonen et al., 2015). The 1644 Ma Suomenniemi batholith is thus identified as one of the earliest (perhaps the earliest) silicic epizonal plutonic precursors that paved the way for the magmatic culmination of the southeastern Finland rapakivi granite system 10-15 m.y. later.

Acknowledgments

This work was funded by the Academy of Finland (grant 1259813 to OTR). We are grateful to Martin Whitehouse, the principal scientist of the NordSIM facility, for excellent collaboration while performing the secondary ion microprobe zircon U-Pb analysis on sample A1042. The NordSIM facility was a jointly funded Nordic infrastructure and this paper is NordSIM publication no. 409. Insightful reviews of the original submission by Eero Hanski and Leonid Shumlyanskyy as well as the Editor-in-Chief of the journal (Jussi Heinonen) improved the paper. Discussions of pertinent matters with Aku Heinonen are greatly appreciated.

References

Alviola, R. 1981. Selostus Mäntyharjun Lovasjärven intruusiota koskevista teollisuusmineraalitutkimuksista vv. 1976–1978. Unpublished report M 19/3132/-81/80, Geological Survey of Finland, 91 p. [in Finnish]

Alviola, R., Johanson, B.S., Rämö, O.T. & Vaasjoki, M. 1999. The Proterozoic Ahvenisto rapakivi granite – massif-type anorthosite complex, southeastern Finland; Petrography and U-Pb chronology. In: Haapala, I. & Rämö, O.T. (Eds.), Rapakivi Granites and Related Rocks. Precambrian Research 95, 89–107. http://dx.doi.org/10.1016/s0301-9268(98)00128-4

Amelin, Yu. & Zaitsev, A.N. 2002. Precise chronology of phoscorites and carbonatites: The critical role of U-series disequilibrium in age interpretations. Geochimica et Cosmochimica Acta 66, 2399–2419. http://dx.doi.org/10.1016/S0016-7037(02)00831-1

Begemann, F., Ludwig, K.R., Lugmair, G.W., Min, K., Nyquist, L.E., Patchett, P.J., Renne, P.R., Shih, C.-Y., Villa, I.M. & Walker, R.J. 2001. Call for an improved set of decay constants for geochronological use. Geochimica et Cosmochimica Acta 65, 111–121. http://dx.doi.org/10.1016/S0016-7037(00)00512-3

Del Moro, A., Puxeddu, M., Radicati di Brozolo, F. & Villa, I.M. 1982. Rb-Sr and K-Ar ages on minerals at temperatures of 300–400°C from deep wells of the Larderello geothermal field (Italy). Contributions to Mineralogy and Petrology 81, 340–349. http://dx.doi.org/10.1007/BF00371688

Dodson, M.H. 1973. Closure temperature in cooling geochronological and petrological systems. Contributions to Mineralogy and Petrology 40, 259–274. http://dx.doi.org/10.1007/BF00373790

Elliott, B.A., Peck, W.H., Rämö, O.T., Vaasjoki, M., Nironen, M. 2005. Magmatic zircon oxygen isotopes of 1.88-1.87 Ga orogenic and 1.65-1.54 Ga anorogenic magmatism in Finland. Mineralogy and Petrology 85, 223–241. http://dx.doi.org/10.1007/s00710-005-0087-3

Emslie, R.F. 1991. Granitoids of rapakivi granite - anorthosite and related associations. In: Haapala, I. & Condie, K.C. (Eds.), Precambrian Granitoids – Petrogenesis, Geochemistry and Metallogeny. Precambrian Research 51, 173–192. http://dx.doi.org/10.1016/0301-9268(91)90100-o

Faure, G. 2001. Origin of Igneous Rocks; The Isotopic Evidence. Springer-Verlag, Berlin, Heidelberg, New York, 501 p. http://dx.doi.org/10.1007/978-3-662-04474-2

Haapala, I. 1997. Magmatic and postmagmatic processes in tin-mineralized granites: topaz-bearing granite in the Eurajoki rapakivi granite stock, Finland. Journal of Petrology 38, 1645–1659. http://dx.doi.org/10.1093/petroj/38.12.1645

Haapala, I. & Rämö, O.T. 1990. Petrogenesis of the Proterozoic rapakivi granites of Finland. In: Stein, H.J. & Hannah, J.L. (Eds.), Ore-Bearing Granite Systems; Petrogenesis and Mineralizing Processes. Geological Society of America Special Paper 246, 275–286. http://dx.doi.org/10.1130/SPE246-p275

Heinonen, A.P., Rämö, O.T., Mänttäri, I., Johanson, B. & Alviola, R. 2010a. Formation and fractionation of high-Al tholeiitic magmas in the Ahvenisto rapakivi granite-massif-type anorthosite complex, southeastern Finland. Canadian Mineralogist 48, 969–990. http://dx.doi.org/10.3749/canmin.48.4.969

Heinonen, A.P., Andersen, T. & Rämö, O.T. 2010b. Re-evaluation of rapakivi petrogenesis: Source contrains from the Hf isotope composition of zircon in the rapakivi granites and associated mafic rocks of southern Finland. Journal of Petrology 51, 1687–1709. http://dx.doi.org/10.1093/petrology/egq035

Heinonen, A., Mänttäri I., Larjamo, K. & Rämö, O.T. 2015. Rapakivi zircon: U-Pb age patterns, chemical composition, and morphology as petrogenetic indicators. In: Kultti, S., Rämö, O.T., Koivisto, E. & Luoto, M. (Eds.), 2nd Finnish National Colloquium of Geosciences, 3.–5.3.2015, Program and Abstracts. Department of Geosciences and Geography C10, Unigrafia, Helsinki, 17.

Johanson, B.S. 1984. Ahvenisto Gabbro-anortositkomplex - en petrografisk och mineralogisk undersökning. Unpublished M.Sc. thesis, University of Helsinki, Department of Geology, 85 p. [in Swedish]

Kohonen, J. 2015. Sedimentary rocks meeting rapakivi granites; one step further towards an overall tectonic model? In: Kultti, S., Rämö, O.T., Koivisto, E. & Luoto, M. (Eds.), 2nd Finnish National Colloquium of Geosciences, 3.-5.3.2015, Program and Abstracts. Department of Geosciences and Geography C10, Unigrafia, Helsinki, 25.

Kohonen, J. & Rämö, O.T. 2005. Sedimentary rocks, diabases and late cratonic evolution. In: Lehtinen, M., Nurmi, P.A. & Rämö, O.T. (Eds.), Precambrian Geology of Finland – Key to the Evolution of the Fennoscandian Shield. Developments in Precambrian Geology, Volume 14. Elsevier, Amsterdam, 563–604. http://dx.doi.org/10.1016/S0166-2635(05)80014-3

Korja, A. & Elo, S. 1990. Crustal and upper mantle structure of the Wiborg batholith, SE Finland. Abstracts of the second symposium on the Baltic shield held in Lund, Sweden, June 5–7, 1990, 57.

Kossert, K. 2003. Half-life measurements of ^{87}Rb by liquid scintillation counting. Applied Radiation and Isotopes 59, 377–382. http://dx.doi.org/10.1016/j.apradiso.2003.08.004

Kouvo, O. 1958. Radioactive age of some Finnish Precambrian minerals. Bulletin de la Comission Géologique de Finlande 182, 70 p.

Krogh, T.E. 1973. A low-contamination method for hydrothermal decomposition of zircon and extraction U and Pb for isotpic age determinations. Geochimica et Cosmochimica Acta 37, 485–494. http://dx.doi.org/10.1016/0016-7037(73)90213-5

Krogh, T.E. 1982. Improved accuracy of U-Pb zircon ages by the creation of more concordant systems using an air abrasion technique. Geochimica et Cosmochimica Acta 46, 637–649. http://dx.doi.org/10.1016/0016-7037(82)90165-X

Lehijärvi, M. & Tyrväinen, A. 1969. Geological map of Finland, 1:100 000, pre-Quaternary rocks, Sheet 3114 Vuohijärvi. Geological Survey of Finland.

Ludwig, K.R. 1991. PbDat 1.21 for MS-dos: A computer program for IBM-PC Compatibles for processing raw Pb-U-Th isotope data. Version 1.07.

Ludwig, K.R. 2003. Isoplot/Ex 3. A geochronological toolkit for Microsoft Excel. Berkeley Geochronology Center. Special publication No. 4.

Lukkari, S. 2007. Magmatic evolution of topaz-bearing granite stocks within the Wiborg rapakivi granite batholith. Publications of the Department of Geology D12, University of Helsinki, Helsinki, 29 p. (plus four article appendices)

Nebel, O., Scherer, E.E. & Mezger, K. 2011. Evaluation of the ^{87}Rb decay constant by age comparison against the U-Pb system. Earth and Planetary Science Letters 301, 1-8. http://dx.doi.org/10.1016/j.epsl.2010.11.004

Neymark, L.A., Amelin, Yu.V. & Larin, A.M. 1994. Pb-Nd-Sr isotopic constraints on the origin on the 1.54-1.56 Ga Salmi rapakivi granite-anorthosite batholith (Karelia, Russia). Haapala, I. & Rämö, O.T. (Eds.), IGCP Project 315 Publication No. 12. Mineralogy and Petrology 50 (1-3), 173–194. http://dx.doi.org/10.1007/bf01160146

Pipping, F. 1956. Rapakivimassivet i Suomenniemi. Unpublished M.Sc. thesis, University of Helsinki, Department of Geology, 53 p. [in Swedish]

Rämö, O.T. 1991. Petrogenesis of the Proterozoic rapakivi granites and related basic rocks of southeastern Fennoscandia: Nd and Pb isotopic and general geochemical constraints. Geological Survey of Finland, Bulletin 355, 161 p.

Rämö, O.T. & Haapala, I. 2005. Rapakivi granites. In: Lehtinen, M., Nurmi, P.A. & Rämö, O.T. (Eds.), Precambrian Geology of Finland – Key to the Evolution of the Fennoscandian Shield. Developments in Precambrian Geology, Volume 14. Elsevier, Amsterdam, 553-562. http:/

/dx.doi.org/10.1016/S0166-2635(05)80013-1

Rämö, O.T., Huhma, H. & Kirs, J., 1996. Radiogenic isotopes of the Estonian and Latvian rapakivi granite suites: new data from the concealed Precambrian of the East European Craton. Precambrian Research 79, 209–226. http://dx.doi.org/10.1016/S0301-9268(95)00083-6

Rämö, O.T., Turkki, V., Mänttäri, I., Heinonen, A.P., Larjamo, K. & Lahaye, Y. 2014. Age and isotopic fingerprints of some plutonic rocks in the Wiborg rapakivi granite batholith with special reference to the dark wiborgite of the Ristisaari Island. Bulletin of the Geological Society of Finland 86, 71–91.

Rämö, T. 1999. Sr isotopic composition of Finnish rapakivi granites: the Suomenniemi batholith. Bulletin of the Geological Society of Finland 71, 339–345.

Rotenberg, E., Davis, D.W., Amelin, Yu., Sanghamitra, G. & Bergquist, B.A. 2012. Determination of the decay-constant of ^{87}Rb by laboratory accumulation of ^{87}Sr. Geochimica et Cosmochimica Acta 85, 41–57. http://dx.doi.org/10.1016/j.gca.2012.01.016

Savolahti, A. 1956. The Ahvenisto massif in Finland. Bulletin de la Commission Géologique de Finlande 174, 96 p.

Shearer, C.K. & Robinson, P. 1988. Petrogenesis of metaluminous and peraluminous tonalities within the Merrimack synclinorium: Harrdwick tonalite, central Massachusetts. American Journal of Science 288-A, 148–195.

Siivola, J. 1987. Lovasjärven mafinen intruusio, the mafic intrusion of Lovasjärvi. In: Aro, K. & Laitakari, I. (Eds.), Suomen diabaasit ja muut mafiset juonikivilajit (Diabases and Other Mafic Dyke Rocks in Finland. Geological Survey of Finland Report of Investigation 76, 121–128. [in Finnish with English Summary]

Simonen, A. & Tyrväinen A. 1981. Savitaipaleen kartta-alueen kallioperä, Pre-Quaternary rocks of the Savitaipale map-sheet area, Geological map of Finland 1:1000,000, Explanation to the map of pre-Quaternary rocks, Sheet 3132. Geological Survey of Finland, 30 p. [in Finnish with English Summary]

Stacey, J.S. & Kramers, J.D. 1975. Approximation of terrestrial lead isotope evolution by a two-stage model. Earth and Planetary Science Letters 26, 207 221. http://dx.doi.org/10.1016/0012-821X(75)90088-6

Steiger, R.H. & Jäger, E. 1977. Subcommission of Geochronology: Convention on the use of decay constants in geo- and cosmochronology. Earth and Planetary Science Letters 36, 359–362. http://dx.doi.org/10.1016/0012-821X(77)90060-7

Sundsten, H. 1985. Suomenniemi rapakivimassivets kontakter, inom kartbladet 3141 Ristiina, Finland. Unpublished M.Sc. thesis, Åbo Akademi University, 42 p. [in Swedish]

Suominen, V. 1991. The chronostratigraphy of SW Finland with special reference to the Postjotnian and Subjotnian diabases. Geological Survey of Finland, Bulletin 356.

Vaasjoki, M. 1977. Rapakivi granites and other postorogenic rocksin Finland: their age and the lead isotopic composition of certainassociated galena mineralizations. Geological Survey of Finland, Bulletin 294, 64 p.

Vaasjoki, M., Rämö, O.T. & Sakko, M. 1991. New U-Pb ages from the Wiborg rapakivi area: constraints on the temporal evolution of the rapakivi granite – anorthosite – diabase dike association of southeastern Finland. Precambrian Research 51, 227–243. http://dx.doi.org/10.1016/0301-9268(91)90102-G

Welin, E., Vaasjoki, M. & Suominen, V., 1983. Age differences between Rb-Sr whole rock and U-Pb zircon ages of syn- and postorogenic Svecokarelian granitoids in Sottunga, SW Finland. Lithos 16, 297–305. http://dx.doi.org/10.1016/0024-4937(83)90017-8

Whitehouse, M.J. & Kamber, B.S. 2005. Assigning dates to thin gneissic veins in high-grade metamorphic terranes: A cautionary tale from Akilia, southwest Greenland. Journal of Petrology 46, 291-318. http://dx.doi.org/10.1093/petrology/egh075

Whitehouse, M.J., Kamber, B.S. & Moorbath, S. 1999. Age significance of U-Th-Pb zircon data from early Archaean rocks of west Greenland – a reassessment based on combined ion microprobe and imaging studies. Chemical Geology 160, 201–224. http://dx.doi.org/10.1016/S0009-2541(99)00066-2

Wiedenbeck, M., Allé, P., Corfu, F., Griffin, W.L., Meier, M., Oberli, F., von Quadt, A., Roddick, J.C. & Spiegel, W. 1995. Three natural zircon standards for U-Th-Pb, Lu-Hf, trace element and REE analyses. Geostandards Newsletter 19, 1–23. http://dx.doi.org/10.1111/j.1751-908X.1995.tb00147.x

York, D. 1969. Least squares fitting of a straight line with correlated errors. Earth and Planetary Science Letters 5, 320-324. http://dx.doi.org/10.1016/S0012-821X(68)80059-7

Zen, E. 1986. Aluminum enrichment in silicate melts by fractional crystallization: Some mineralogic and petrographic constraints. Journal of Petrology 27, 1095-1117. http://dx.doi.org/10.1093/petrology/27.5.1095

Table A1. Multigrain isotope-dilution zircon U-Pb isotopic data for samples A1042, A1043, and A1130 from the granites and samples A0021, A0099, A1100, and A1163 from the quartz-feldspar porphyry dikes of the Suomenniemi complex (courtesy of the Geological Survey of Finland; see also Vaasjoki et al., 1991, Tables 2 and 3)

Sample information	Sample	^{238}U	^{206}Pb	$^{206}Pb/^{204}Pb$	$^{208}Pb/^{206}Pb$	ISOTOPIC RATIOS[1]						Rho[2]	APPARENT AGES/Ma±2σ		
Analysed mineral and fraction	mg	ppm	ppm	measured	radiogenic	$^{206}Pb/^{238}U$	±2σ%	$^{207}Pb/^{235}U$	±2σ%	$^{207}Pb/^{206}Pb$	±2σ%		$^{206}Pb/^{238}U$	$^{207}Pb/^{235}U$	$^{207}Pb/^{206}Pb$
A1402 Uiruvuori biotite granite															
A) +4.3/-160 µm	11.4	381	74	960	0.26	0.2233	0.62	3.080	0.62	0.1001	0.17	0.96	1299	1427	1625±3
B) 4.2-4.3/-160 µm	10.4	718	140	790	0.26	0.2250	0.66	3.112	0.67	0.1003	0.24	0.93	1308	1435	1629±4
C) +4.3/+160 µm/abr	6.6	317	73	1506	0.21	0.2674	0.62	3.710	0.62	0.1006	0.34	0.85	1527	1573	1636±7
D) +4.3/+160 µm	5.8	376	75	675	0.27	0.2322	0.65	3.206	0.65	0.1001	0.37	0.84	1346	1458	1626±7
E) 4.0-4.2/80-160 µm	7.0	980	182	1129	0.22	0.2152	0.72	2.9505	0.72	0.0994	0.25	0.94	1256	1394	1613±5
A1043 Pohjalampi hornblende granite															
A) +4.3/80-160 µm/abr 3h	18.9	258	58	3099	0.10	0.2582	0.65	3.570	0.65	0.1003	0.21	0.95	1480	1542	1629±4
B) +4.3/80-160 µm	12.0	251	56	2929	0.10	0.2577	0.57	3.562	0.58	0.1003	0.31	0.85	1477	1541	1629±6
C) 4.2-4.3/+80 µm	10.9	638	116	1954	0.10	0.2097	0.76	2.852	0.76	0.0986	0.23	0.96	1227	1369	1598±4
D) 4.0-4.2/+80 µm	5.1	802	133	1397	0.10	0.1922	0.55	2.5956	0.56	0.0979	0.24	0.91	1133	1299	1585±5
E) +4.3/80-160 µm/abr 6h	9.8	186	46	2294	0.11	0.2845	0.98	3.954	0.98	0.1008	0.34	0.94	1614	1624	1638±6
A1130 Sikolampi hornblende-augite-fayalite granite															
A) +4.3/abr 3h	10.2	260	25	197	0.50	0.1129	0.71	1.482	0.72	0.0952	0.77	0.42	689	922	1531±15
B) 4.3-4.5/+160 µm	12.9	1167	65	218	0.31	0.0644	1.49	0.814	1.49	0.0917	0.32	0.98	402	604	1461±6
C) 4.2-4.3/+160 µm	12.3	526	128	4526	0.17	0.2818	0.56	3.907	0.62	0.1006	0.27	0.90	1600	1615	1634±5
D) 4.0-4.2/+160 µm	8.3	618	148	2369	0.17	0.2764	0.85	3.838	0.85	0.1007	0.15	0.98	1573	1600	1637±3
E) +4.3/+160 µm/abr	10.1	254	59	11359	0.15	0.2666	0.76	3.7098	0.78	0.1009	0.18	0.97	1523	1573	1641±4
F) +4.5/-160 µm	4.2	425	28	352	0.76	0.0773	0.71	1.014	0.71	0.0952	0.41	0.83	479	710	1531±8
A0099 Kiesilä quartz-feldspar porphyry dike															
A) +4.3/HF	15.0	230	37	759	0.32	0.1844	0.58	2.503	0.76	0.0984	0.43	0.83	1091	1272	1594±10
B) +4.3	17.2	306	41	605	0.38	0.1544	0.54	2.043	0.68	0.0960	0.37	0.84	925	1130	1548±9
C) 4.2-4.3/HF	15.8	648	110	1495	0.29	0.1961	0.62	2.642	0.73	0.0977	0.34	0.89	1154	1312	1581±9
D) +4.3/HF/crushed	20.2	156	34	2024	0.24	0.2488	0.64	3.428	1.05	0.0999	0.75	0.70	1432	1510	1622±16

A1100 Nikkari quartz-feldspar porphyry dike														
A) +4.6/+160 µm/abr	6.8	101	25	2193	0.17	0.2833	0.60	3.929	0.60	0.1006	0.59	0.52	1608	1619	1635±11
B) +4.6/+160 µm	5.6	112	26	1710	0.18	0.2701	0.65	3.742	0.66	0.1005	0.73	0.39	1541	1580	1633±13
C) 4.3-4.5/+160 µm	5.5	181	41	1047	0.20	0.2645	0.68	3.668	0.69	0.1006	0.49	0.74	1512	1564	1634±9
A1163 Viitalampi quartz-feldspar porphyry dike															
A) +4.5 /abr	11.8	44	11	585	0.27	0.2836	0.80	3.939	0.81	0.1007	0.55	0.77	1609	1621	1638±10
B) +4.5	10.6	56	12	477	0.29	0.2484	0.81	3.471	0.82	0.1013	0.84	0.47	1430	1520	1649±16
C) 4.3-4.5/+160 µm	10.4	64	14	210	0.38	0.2543	1.76	3.531	1.76	0.1007	0.33	0.98	1460	1534	1637±6
A0021 Mentula quartz-feldspar porphyry dike															
A) 3.8-4.1	13.8	1176	210	585	0.28	0.2064	0.59	2.817	0.66	0.0990	0.25	0.93	1209	1360	1605±7
B) +4.6 /HF/crushed	20.1	110	27	4375	0.23	0.2815	0.64	3.901	0.68	0.1005	0.16	0.97	1598	1613	1633±4
C) +4.6	21.9	142	27	705	0.28	0.2225	0.72	3.065	0.86	0.0999	0.43	0.87	1294	1424	1623±10
D) 4.4-4.6/80-160 µm	21.0	332	60	815	0.27	0.2094	0.66	2.867	0.76	0.0993	0.32	0.91	1225	1373	1611±8
E) +4.6 /HF	20.0	113	26	740	0.27	0.2640	0.64	3.669	1.33	0.1008	1.05	0.63	1510	1564	1639±21

1) Isotopic ratios corrected for fractionation, blank (30 or 50 pg), and age related common lead (Stacey & Kramers 1975). 2) Rho: Error correlation between $^{206}Pb/^{238}U$ and $^{207}Pb/^{235}U$ ratios. All errors are 2σ.

Analytical methods: The decomposition of zircon and extraction of U and Pb for multigrain ID-TIMS (isotope dilution - thermal ionisation mass spectrometry) isotopic age determinations follows mainly the procedure described by Krogh (1973, 1982). ^{235}U-^{208}Pb-spiked and unspiked isotope ratios were measured using a VG Sector 54 thermal ionization multicollector mass spectrometer. According to repeated measurements of Pb standard SRM981, the measured lead isotopic ratios were corrected for 0.12-0.10±0.05% / a.m.u. fractionation. Pb/U ratios were calculated using PbDat-program (Ludwig, 1991). Plotting of the isotopic data and age calculations were done using Isoplot/Ex 3 program (Ludwig, 2003). Age errors are calculated at 2σ and decay constants errors ignored. Data-point error ellipses in figures are 2σ.